machines

MDPI

Article

Add-On Type Data-Driven Ripple-Free Dual-Rate Control Design Based on the Null Space of Steady-State Step Responses

Takao Sato *, Ryota Yasui and Natsuki Kawaguchi

Graduate School of Engineering, University of Hyogo, 2167 Shosha, Himeji 671-2280, Hyogo, Japan; ryotay1953@gmail.com (R.Y.); kawaguchi@eng.u-hyogo.ac.jp (N.K.)
* Correspondence: tsato@eng.u-hyogo.ac.jp; Tel.: +81-792674983

Abstract: In the present study, a data-driven ripple-free design is proposed for a dual-rate sampled-data control system in which the sampling interval of the plant output is longer than the holding interval of the control input. The objective of the present study is to improve the steady-state intersample response without changing the sampled response and without using the plant model. To achieve the objective directly from controlled data, an add-on input based on the null space of steady-state step responses to an existing control system is used. The open-loop or closed-loop system to obtain the step response is assumed to be stable. In the present study, a two-degree-of-freedom design is given that redesigns the intersample output response independently of the steady-state sampled output response. In a numerical example, the proposed method is applied to a linear time-invariant single-input single-output stable system, where intersample ripples are eliminated using the add-on input that is independent of the existing sample output response in steady state.

Keywords: data-driven; sampled-data control; dual-rate; intersample ripple; add-on input; step response

check for updates

Citation: Sato, T.; Yasui, R.; Kawaguchi, N. Add-On Type Data-Driven Ripple-Free Dual-Rate Control Design Based on the Null Space of Steady-State Step Responses. *Machines* **2022**, *10*, 296. https://doi.org/10.3390/machines10050296

Academic Editor: Dan Zhang

Received: 25 February 2022
Accepted: 20 April 2022
Published: 22 April 2022

1. Introduction

Most recent control systems are implemented using digital computers in the discrete-time domain. When a continuous-time plant is controlled by a digital computer, it is designed as a sampled-data control system [1,2] where the continuous-time signal is sampled by a sampler and the discrete-time signal is held by a holder. When the sampling interval of plant outputs and the holding interval of control inputs are equal, the designed system is referred to as a single-rate system; otherwise, it is referred to as a multi-rate or dual-rate system [3–6]. Although the control design of a dual-rate system is more complex than that of a single-rate system, the control performance of a dual-rate system is better than that of a single-rate system when the sampling, holding, or both intervals are limited. Examples of applications of dual-rate systems include distillation column compositions [7], DC-AC converters [8], network control systems [9], and hard disk drives [10–12].

Dual-rate control, which is difficult to design because it is a time-varying system, is designed as a multi-variable time-invariant system by using lifting techniques [1,13,14]. Because of the high performance of recent digital computers, the update of a control input is often shorter than the sampling of a plant output. In such a dual-rate sampled-data control system, the control input, which is essentially a single signal, can be designed independently as a multi-input. Considering a single-input single-output (SISO) system as an example, the system can be viewed as a multi-input single-output system where the input signals are switched in time, as shown in Figure 1. In such a dual-rate system, as shown in Figure 2, because the time-switching control input is redundant with respect to the discrete-time output, the discrete-time output from that control input is not uniquely determined. As a result, because the control input may change between sampling instants,

the intersample output might oscillate even if the plant output converges to the reference input at sampling instants [15–19]. The intersample ripple caused by the input oscillation is eliminated when the ripple-free condition is satisfied [20]. Ripple attenuation methods have been proposed in which this condition is not used [21–23]. However, a discrete-time model is needed to design feedforward and feedback controllers [21]; the frequency information for high-frequency disturbances is required to attenuate the intersample oscillation caused by disturbances [22] and a continuous-time dynamic model is needed to minimize the intersample control error [23]. The ripple-free condition is thus useful for solving the intersample ripple problem without the need for plant models or disturbance information. Because discrete-time sample performance is as important as intersample performance, the degradation of the sample performance of an existing system due to the elimination of intersample ripple must be prevented. For example, in the position control of the head in a hard disk drive, the head must follow the target position in the discrete-time domain to read and write user data [10,11]. To this end, a two-degree-of-freedom design in which intersample ripple is eliminated independently of the discrete-time performance is ideal [24].

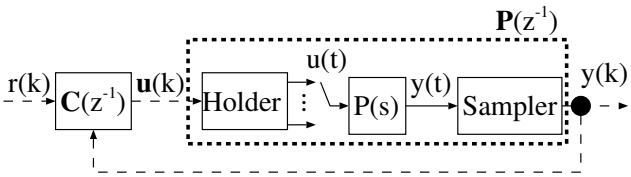

Figure 1. Block diagram of a dual-rate sampled-data system.

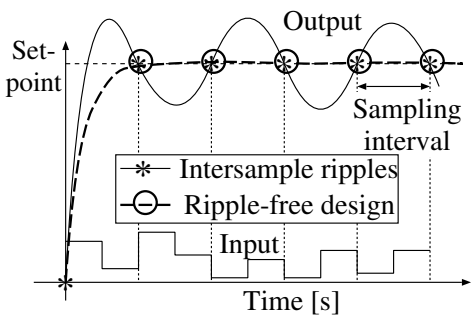

Figure 2. Trajectories with and without ripple.

A redundancy-based continuous-time-domain approach has been proposed [25]. In the method, a redundant variable is introduced based on the redundancy of a controlled plant model and used to reassign control inputs independently of the plant output. A discrete-time-domain method for redundant control design has also been proposed [26–28]. In continuous-time-domain design methods, the presence of redundancy depends on the controlled plant structure, whereas in discrete-time-domain design methods, because dual-rate systems are designed, redundancy is achieved even if the controlled plant is a non-redundant system.

Most ripple-free control methods adopt the model-based approach, whereas there is a data-driven (model-free) method [14,29]. In the conventional model-free method, only stable systems can be applied since open-loop control is executed for controller parameter tuning. Furthermore, a control system is newly designed, and hence the sample performance of an existing system is not maintained. In the conventional model-based dual-rate design method [26], a redundant variable is designed so that intersample ripple is eliminated in the steady state. Because the redundant variable is independent of the sampled plant output, intersample ripple is eliminated without changing the sampled output obtained by an existing control system, as shown in Figure 2. When the goal of the design is to eliminate the steady-state intersample ripple, it can be achieved by simply using steady-state characteristics (i.e., not all dynamic characteristics are required).

Furthermore, because the steady-state characteristics of dual-rate systems can be identified by step responses, a model-free ripple-free design is also realizable. Therefore, in the present study, a model-free method for independently removing intersample ripple from the steady-state discrete-time output response is discussed. Specifically, the redundant variable is designed based on the null space of steady-state step responses. The step response is not a problem if the plant is stable, while if it is unstable, bounded values cannot be obtained. In the proposed method, since the add-on input is designed as long as bounded step responses are obtained in the steady state, both open-loop and closed-loop responses can be used. Therefore, for unstable plants, the proposed method is designed using stabilized closed-loop responses instead of open-loop responses. As a result, the proposed method is applicable to unstable plants as well as stable plants.

The rest of this paper is organized as follows: Section 2 describes a dual-rate sampled-data control system, and Section 3 describes the design method of an add-on input independent of the steady-state sampled plant output using step responses. The effectiveness of the proposed method is then shown in Section 4. Finally, conclusions are presented in Section 5. In the present study, z^{-1} denotes the backward shift operator, and $\boldsymbol{I}_n$ and $\boldsymbol{0}_{m,n}$ are an $n \times n$ identity matrix and an $m \times n$ zero matrix, respectively. $\mathbb{N}^+$ and $\mathbb{R}^+$ denote the spaces of positive integer and positive real numbers, respectively, and $\mathbb{R}$ denotes the space of real numbers. Lightface denotes a scalar, and boldface denotes a vector or matrix.

2. Problem Statement

The controlled plant is assumed to be an SISO linear time-invariant continuous-time system. Because the plant is controlled by a digital computer in the discrete-time domain, the continuous-time plant output is sampled and converted to a discrete-time signal, and the discrete-time control input calculated by the digital computer is held and converted to a continuous-time signal. The holding and sampling intervals are assumed to be as follows.

Assumption 1.

1. *The holding interval T is known.*
2. *The sampling interval lT is known.*

where $T \in \mathbb{R}^+$ and $l \in \mathbb{N}^+$. If the continuous-time plant output is sampled at intervals of T, the single-rate system is obtained:

$$y(k) = P(z^{-1})u(k) \tag{1}$$

where $y(k) \in \mathbb{R}$ and $u(k) \in \mathbb{R}$ are the sampled plant output and discrete-time control input, respectively, and $P(z^{-1})$ is the transfer function in the discrete-time domain.

With Assumption 1, the controlled plant is modeled as a dual-rate system as follows [17,20]:

$$\begin{aligned} y(k) &= \boldsymbol{P}(z^{-1})^\top \boldsymbol{u}(k-l) \\ \boldsymbol{P}(z^{-1}) &= [P_1(z^{-1}) \;\; P_2(z^{-1}) \;\; \cdots \;\; P_l(z^{-1})]^\top \\ \boldsymbol{u}(k) &= [u(k) \;\; u(k+1) \;\; \cdots \;\; u(k+l-1)]^\top \\ &= [u_1(k) \;\; u_2(k) \;\; \cdots \;\; u_l(k)]^\top \\ u_i(k) &= u(k+i-1) \;\; (i = 1, \cdots, l) \end{aligned} \tag{2}$$

Assumption 2.

1. *$P(z^{-1})$ has no zero at the origin.*
2. *$P(z^{-1})$ and $\boldsymbol{P}(z^{-1})$ are unknown.*

A dual-rate control system is designed using the following control law:

$$\boldsymbol{Y}(z^{-1})\boldsymbol{u}(k) = \boldsymbol{K}(z^{-1})r(k) - \boldsymbol{X}(z^{-1})y(k) \tag{3}$$

where $r(k) \in \mathbb{R}$ is the reference input for the plant output and is set to a step function. $\boldsymbol{K}(z^{-1})$ and $\boldsymbol{X}(z^{-1})$ are polynomial vectors and $\boldsymbol{Y}(z^{-1})$ is a non-singular polynomial matrix.

Using the discrete-time control law, the closed-loop system from the reference input to the plant output is given as follows:

$$y(k) = z^{-l}\boldsymbol{G}(z^{-1})^{\top}\boldsymbol{K}(z^{-1})r(k) \tag{4}$$

$$\boldsymbol{G}(z^{-1})^{\top} = \frac{\boldsymbol{P}(z^{-1})^{\top}\boldsymbol{Y}(z^{-1})^{-1}}{1 + z^{-l}\boldsymbol{P}(z^{-1})^{\top}\boldsymbol{Y}(z^{-1})^{-1}\boldsymbol{X}(z^{-1})} \tag{5}$$

A block diagram of the designed dual-rate control system is shown in Figure 3.

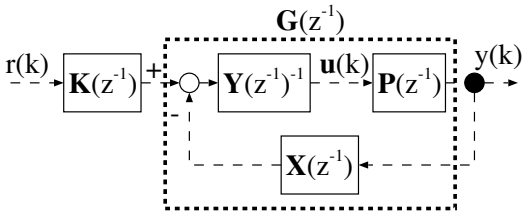

Figure 3. Block diagram of dual-rate sampled-data control system.

Assumption 3. *For the closed-loop system, the following conditions are satisfied.*

1. *The closed-loop system described by Equation (4) is stable.*
2. *The steady-state discrete-time output converges to the reference input.*
3. *The closed-loop transfer function $\boldsymbol{G}(z^{-1})$ is unknown.*

Because the closed-loop system is stable from Assumption 3, the steady-state plant output is calculated as follows:

$$y(\infty) = \boldsymbol{G}(1)^{\top}\boldsymbol{K}(1)r(\infty) \tag{6}$$

The closed-loop system from the reference input to the control input vector is given as follows:

$$\boldsymbol{u}(k) = \boldsymbol{G}_r(z^{-1})r(k) \tag{7}$$

$$\boldsymbol{G}_r(z^{-1}) = (\boldsymbol{Y}(z^{-1}) + z^{-l}\boldsymbol{X}(z^{-1})\boldsymbol{P}(z^{-1})^{\top})^{-1}\boldsymbol{K}(z^{-1}) \tag{8}$$

When the control input is constant between sampling instants, there is no intersample ripple in the steady state [20]. The ripple-free condition is therefore described as follows:

$$u_i(\infty) = u_{i+1}(\infty) \;\; (i = 1, 2, \cdots, l-1) \tag{9}$$

If the control law is redesigned so as to satisfy the above condition, the existing correctly calibrated sampled response may degrade. In the next section, to prevent such degradation, the control law is extended using the null space and the ripple-free condition is then satisfied independently of the existing steady-state discrete-time response. As a result, intersample ripple is eliminated independently of the steady-state discrete-time response.

3. Ripple-Free Design Using Add-On Input

3.1. Extended Control Law Using Null Space of Step Responses

First, matrix $\boldsymbol{G}_{\perp}$ is defined as follows.

Definition 1. *$\boldsymbol{G}_\perp$ satisfies the following relational expressions:*

$$Im(\boldsymbol{G}_\perp) = Ker(\hat{\boldsymbol{G}}(1)^\top)$$
$$Ker(\hat{\boldsymbol{G}}(1)^\top) := \{\boldsymbol{G}_\perp \in \mathbb{R}^{l\times l-1} \mid \hat{\boldsymbol{G}}(1)^\top \boldsymbol{G}_\perp = \boldsymbol{0}_{1,l-1}\}$$

where $\hat{\boldsymbol{G}}(1)$ denotes the identified value of $\boldsymbol{G}(1)$. The i-th element of $\boldsymbol{G}(1)$ can be identified by the steady-state value of the step response of Equation (6) when the elements of $\boldsymbol{K}(z^{-1})$, excluding the i-th element, are set to 0. $\boldsymbol{P}(z^{-1})$ is unknown, whereas $\hat{\boldsymbol{G}}(1)$ is available, and thus $\boldsymbol{G}_\perp$ that satisfies Definition 1 is obtained.

Using $\boldsymbol{G}_\perp$, the control law is extended as follows:

$$\boldsymbol{Y}(z^{-1})\boldsymbol{u}(k) = \boldsymbol{K}(z^{-1})r(k) - \boldsymbol{X}(z^{-1})y(k) + \boldsymbol{G}_\perp \boldsymbol{w}(k) \tag{10}$$

where $\boldsymbol{w}(k) \in \mathbb{R}^{l-1}$ is an add-on input. The block diagram of the extended system is shown in Figure 4. The closed-loop system that uses the extended control law is given as follows:

$$y(k) = z^{-l}\boldsymbol{G}(z^{-1})^\top \boldsymbol{K}(z^{-1})r(k) + z^{-l}\boldsymbol{G}(z^{-1})^\top \boldsymbol{G}_\perp \boldsymbol{w}(k) \tag{11}$$

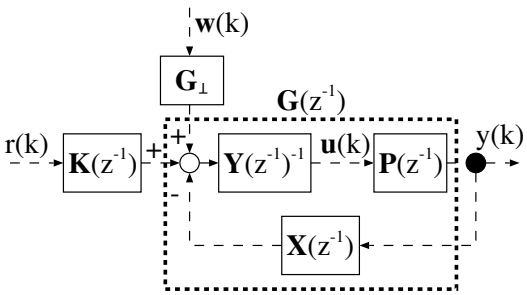

Figure 4. Block diagram of extended system.

In the steady state, the output response is obtained as follows:

$$y(\infty) = \boldsymbol{G}(1)^\top \boldsymbol{K}(1)r(\infty) + \boldsymbol{G}(1)^\top \boldsymbol{G}_\perp \boldsymbol{w}(\infty) \tag{12}$$

In the above equation, the second term on the right-hand side is always 0 for the bounded $\boldsymbol{w}(\infty)$ from Definition 1 when $\boldsymbol{G}(1) = \hat{\boldsymbol{G}}(1)$, and $\boldsymbol{w}(\infty)$ is independent of the steady-state sampled output obtained using Equation (3). Therefore, the steady-state sampled response, Equation (6), is maintained even when the extended control law is applied. Furthermore, using the add-on input, intersample ripple is eliminated without changing the steady-state sampled output response. In Section 3.2, $\boldsymbol{w}(k)$ is designed to satisfy the ripple-free condition in Equation (9).

3.2. Design of Add-On Input

The closed-loop system from both the reference and the add-on input to the control input vector is obtained as follows:

$$\boldsymbol{u}(k) = \boldsymbol{G}_r(z^{-1})r(k) + \boldsymbol{G}_w(z^{-1})\boldsymbol{w}(k) \tag{13}$$
$$\boldsymbol{G}_w(z^{-1}) = (\boldsymbol{Y}(z^{-1}) + z^{-l}\boldsymbol{X}(z^{-1})\boldsymbol{P}(z^{-1})^\top)^{-1}\boldsymbol{G}_\perp \tag{14}$$

In the steady state, Equation (13) is described as follows:

$$\boldsymbol{u}(\infty) = \boldsymbol{G}_r(1)r(\infty) + \boldsymbol{G}_w(1)\boldsymbol{w}(\infty) \tag{15}$$

Because the unknown $\boldsymbol{P}(1)$ is included in both $\boldsymbol{G}_r(1)$ and $\boldsymbol{G}_w(1)$, these cannot be straightforwardly calculated. The present study proposes a lemma to obtain $\boldsymbol{G}_r(1)$ and $\boldsymbol{G}_w(1)$ without using $\boldsymbol{P}(1)$.

Lemma 1. *Using $\hat{\boldsymbol{G}}(1)$, $\boldsymbol{G}_r(1)$ and $\boldsymbol{G}_w(1)$ are calculated as follows:*

$$\boldsymbol{G}_r(1) = \boldsymbol{Y}(1)^{-1}(\boldsymbol{I}_l - \boldsymbol{X}(1)\hat{\boldsymbol{G}}(1)^\top)\boldsymbol{K}(1) \tag{16}$$

$$\boldsymbol{G}_w(1) = \boldsymbol{Y}(1)^{-1}(\boldsymbol{I}_l - \boldsymbol{X}(1)\hat{\boldsymbol{G}}(1)^\top)\boldsymbol{G}_\perp \tag{17}$$

Proof. From the matrix inversion lemma,

$$\begin{aligned}
&(\boldsymbol{Y}(1) + \boldsymbol{X}(1)\boldsymbol{P}(1)^\top)^{-1} \\
&= \boldsymbol{Y}(1)^{-1} - \boldsymbol{Y}(1)^{-1}\boldsymbol{X}(1)(1 + \boldsymbol{P}(1)^\top\boldsymbol{Y}(1)^{-1}\boldsymbol{X}(1))^{-1}\boldsymbol{P}(1)^\top\boldsymbol{Y}(1)^{-1} \\
&= \boldsymbol{Y}(1)^{-1} - \boldsymbol{Y}(1)^{-1}\boldsymbol{X}(1)\boldsymbol{G}(1)^\top
\end{aligned} \tag{18}$$

where $\boldsymbol{G}(1)$ is given by Equation (5) as follows:

$$\boldsymbol{G}(1)^\top = (1 + \boldsymbol{P}(1)^\top\boldsymbol{Y}(1)^{-1}\boldsymbol{X}(1))^{-1}\boldsymbol{P}(1)^\top\boldsymbol{Y}(1)^{-1} \tag{19}$$

Substituting Equation (18) into Equations (8) and (14) in the steady state, respectively, and using $\hat{\boldsymbol{G}}(1)$ instead of $\boldsymbol{G}(1)$, Equations (16) and (17) are obtained. □

$\boldsymbol{Y}(1)$, $\boldsymbol{X}(1)$ and $\boldsymbol{K}(1)$ are the design parameters of the control law, and $\boldsymbol{G}_\perp$ is decided based on $\hat{\boldsymbol{G}}(1)$. Therefore, $\boldsymbol{G}_r(1)$ and $\boldsymbol{G}_w(1)$ are obtained even when the plant model is unknown.

Theorem 1. *The ripple-free condition is satisfied when $\boldsymbol{w}(\infty)$ is designed as follows:*

$$\boldsymbol{w}(\infty) = -\bar{\boldsymbol{G}}_w^{-1}\bar{\boldsymbol{G}}_r r(\infty) \tag{20}$$

where $\bar{\boldsymbol{G}}_w$ and $\bar{\boldsymbol{G}}_r$ are given as follows:

$$\begin{aligned}
\bar{\boldsymbol{G}}_w &= \boldsymbol{G}_w^u - \boldsymbol{G}_w^l \\
\boldsymbol{G}_w^u &= [I_{l-1} \;\; \boldsymbol{0}_{l-1,1}]\boldsymbol{G}_w(1) \\
\boldsymbol{G}_w^l &= [\boldsymbol{0}_{l-1,1} \;\; I_{l-1}]\boldsymbol{G}_w(1) \\
\bar{\boldsymbol{G}}_r &= \boldsymbol{G}_r^u - \boldsymbol{G}_r^l \\
\boldsymbol{G}_r^u &= [I_{l-1} \;\; \boldsymbol{0}_{l-1,1}]\boldsymbol{G}_r(1) \\
\boldsymbol{G}_r^l &= [\boldsymbol{0}_{l-1,1} \;\; I_{l-1}]\boldsymbol{G}_r(1)
\end{aligned}$$

Proof. From Equation (15), the steady-state control input between the sampling instants is given as follows:

$$\underbrace{\begin{bmatrix} u_1(\infty) \\ u_2(\infty) \\ \vdots \\ u_l(\infty) \end{bmatrix}}_{\boldsymbol{u}(\infty)} = \underbrace{\begin{bmatrix} g_{r_1} \\ g_{r_2} \\ \vdots \\ g_{r_l} \end{bmatrix}}_{\boldsymbol{G}_r(1)} r(\infty) + \underbrace{\begin{bmatrix} g_{w_{1,1}} & g_{w_{1,2}} & \cdots & g_{w_{1,l-1}} \\ g_{w_{2,1}} & g_{w_{2,2}} & \cdots & g_{w_{2,l-1}} \\ \vdots & & & \vdots \\ g_{w_{l,1}} & g_{w_{l,2}} & \cdots & g_{w_{l,l-1}} \end{bmatrix}}_{\boldsymbol{G}_w(1)} \underbrace{\begin{bmatrix} w_1(\infty) \\ w_2(\infty) \\ \vdots \\ w_{l-1}(\infty) \end{bmatrix}}_{\boldsymbol{w}(\infty)} \tag{21}$$

For $u_i(\infty) = u_{i+1}(\infty)$, the next equation must be satisfied:

$$\begin{bmatrix} g_{w_{i,1}} - g_{w_{i+1,1}} & g_{w_{i,2}} - g_{w_{i+1,2}} & \cdots & g_{w_{i,l-1}} - g_{w_{i+1,l-1}} \end{bmatrix}\boldsymbol{w}(\infty) = -(g_{r_i} - g_{r_{i+1}})r(\infty) \tag{22}$$

From the above condition, all the conditions from $i = 1$ to $i = l - 1$ are summarized as follows:

$$\bar{\boldsymbol{G}}_w \boldsymbol{w}(\infty) = -\bar{\boldsymbol{G}}_r r(\infty) \tag{23}$$

As a result, the design condition (20) is obtained. □

Corollary 1. *If the controlled plant is stable, the identified steady-state plant gain $\hat{\boldsymbol{P}}(1)$ is also obtained by step responses. Based on the null space of $\hat{\boldsymbol{P}}(1)$, the control law Equation (3) can be extended as follows:*

$$\boldsymbol{Y}(z^{-1})\boldsymbol{u}(k) = \boldsymbol{K}(z^{-1})r(k) - \boldsymbol{X}(z^{-1})y(k) + \boldsymbol{Y}(z^{-1})\boldsymbol{P}_\perp \boldsymbol{w}_o(k) \tag{24}$$

where $\boldsymbol{w}_o(k) \in \mathbb{R}^{l-1}$ is a new add-on input, and a non-zero matrix $\boldsymbol{P}_\perp \in \mathbb{R}^{l \times l-1}$ is derived that satisfies the following equation:

$$\hat{\boldsymbol{P}}(1)^\top \boldsymbol{P}_\perp = \boldsymbol{0}_{1,l-1} \tag{25}$$

Using the extended control law Equation (24), the corresponding closed-loop system is given as follows:

$$y(k) = \boldsymbol{G}(z^{-1})^\top \boldsymbol{K}(z^{-1})r(k) + \frac{\boldsymbol{P}(z^{-1})^\top \boldsymbol{Y}(z^{-1})^{-1}\boldsymbol{Y}(z^{-1})\boldsymbol{P}_\perp}{1 + z^{-l}\boldsymbol{P}(z^{-1})^\top \boldsymbol{Y}(z^{-1})^{-1}\boldsymbol{X}(z^{-1})}\boldsymbol{w}_o(k) \tag{26}$$

In the steady state, because the second term on the right-hand side of Equation (26) is 0, $\boldsymbol{w}_o(\infty)$ is independent of the steady-state output of Equation (4). $\boldsymbol{w}_o(\infty)$ is therefore designed in the same way as Theorem 1 so that intersample ripple is eliminated without changing the steady-state sampled output. However, the open-loop design method requires a plant model and is not applicable to unstable plants.

4. Simulation

To demonstrate the effectiveness of the proposed closed-loop-based method, two types of plant are controlled, namely stable and unstable plants. In the simulation, the reference input is given by set-point 1, and the holding and sampling intervals are set as 1 s and 2 s ($l = 2$), respectively.

4.1. Stable Plant

As a controlled plant, the following stable continuous-time system is given:

$$P(s) = \frac{1}{s^2 + 3s + 1} \tag{27}$$

The dual-rate model is described as follows:

$$\begin{aligned} \boldsymbol{P}(z^{-1}) &= [P_1(z^{-1}) \;\; P_2(z^{-1})]^\top \\ P_1(z^{-1}) &= \frac{0.242 + 0.00403z^{-2}}{1 - 0.471z^{-2} + 0.00248z^{-4}} \\ P_2(z^{-1}) &= \frac{0.213 + 0.00718z^{-2}}{1 - 0.471z^{-2} + 0.00248z^{-4}} \end{aligned} \tag{28}$$

The coefficients of the control law Equation (3) are designed as follows:

$$\boldsymbol{Y}(z^{-1}) = \begin{bmatrix} 1.0 + 0.0396z^{-2} & -0.100z^{-2} \\ 0 & 1 \end{bmatrix}$$
$$\boldsymbol{K}(z^{-1}) = \begin{bmatrix} 1.68 \\ 1.68 \end{bmatrix}$$
$$\boldsymbol{X}(z^{-1}) = \begin{bmatrix} 1.06 - 0.735z^{-2} \\ 1 \end{bmatrix}$$

where the poles of the designed closed-loop characteristic polynomial are 4.45×10^{-3}, 0.271 and -0.315, and the steady-state gain from the reference input to the plant output is 1.

First, the control result obtained using the control law in Equation (3) with the coefficients designed as described above is shown in Figures 5–7, where the output and input trajectories are plotted by the black dashed-dotted lines, and the sampled output trajectory is plotted by black '*' symbols. It can be seen that the intersample output oscillates even though the sampled output converges to the reference input. This is because the steady-state gain $\boldsymbol{G}_r(1)$ is $[1.37 \;\; 0.683]^\top$, and the control input is thus not constant, even though the control error between the reference input and the sampled plant output is 0.

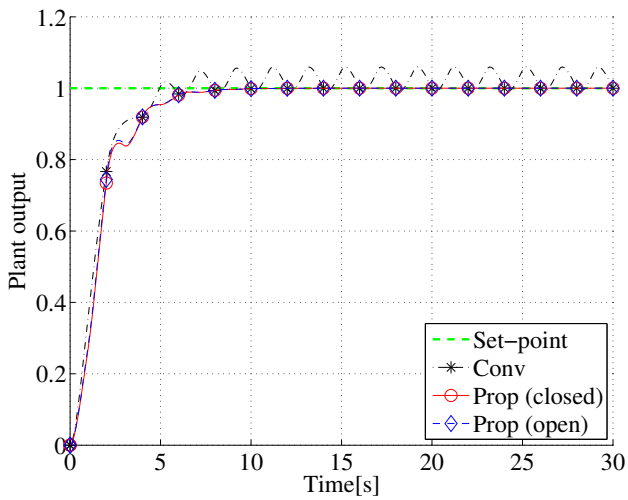

Figure 5. Output trajectories of stable plant.

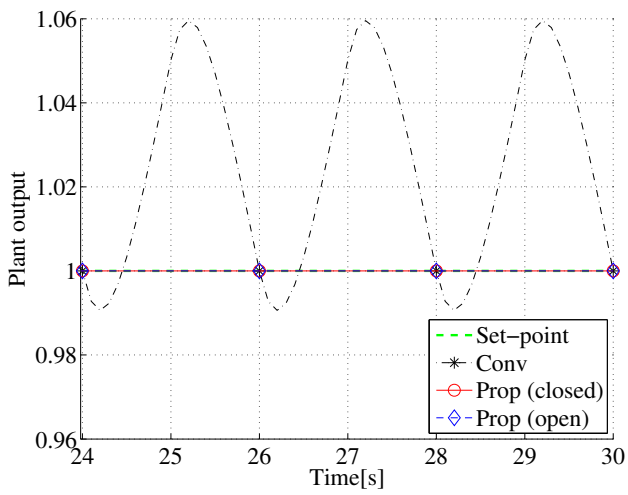

Figure 6. Steady-state trajectories for data in Figure 5.

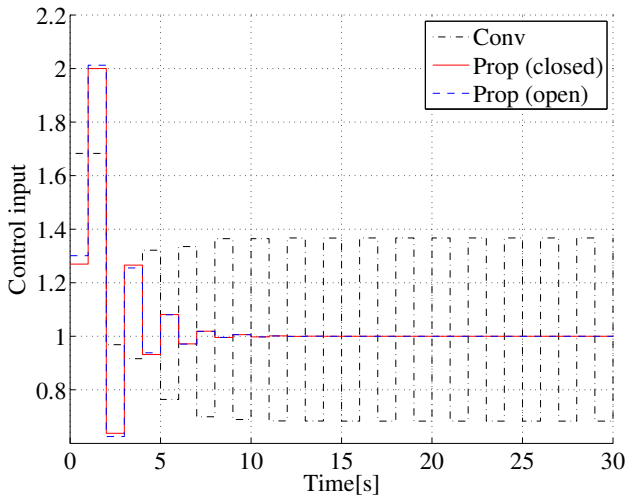

Figure 7. Input trajectories for stable plant.

Second, the simulation result for the proposed method is presented. From two close-loop step responses of 50 s, where $\boldsymbol{K}(z^{-1})$ is set to $[1\ 0]^\top$ and $[0\ 1]^\top$, respectively, the steady-state gain of the closed-loop system is identified as follows:

$$\hat{\boldsymbol{G}}(1) = \begin{bmatrix} 0.258 & 0.336 \end{bmatrix}^\top$$

The vector orthogonal to the steady-state gain is decided as follows:

$$\boldsymbol{G}_\perp = \begin{bmatrix} -0.794 & 0.609 \end{bmatrix}^\top$$

Using Equation (20), the add-on input $w(k)$ is designed as follows:

$$w(k) = w(\infty) = 0.521 \tag{29}$$

Equation (29) shows that $w(k)$ is designed as a constant. The control result obtained using the proposed closed-loop-based extension method is also shown in Figures 5–7, where the output and input trajectories are plotted by the red solid lines, and the sampled output trajectory is plotted by red '$\circ$' symbols. It can be seen that the intersample output as well as the sampled output converge to the reference input without intersample ripple. Furthermore, the sampled output response obtained by the conventional non-extension method is maintained in the steady state even though the trajectories of the control inputs obtained by the proposed and conventional methods are quite different.

Third, for comparison with the proposed closed-loop-based extension method, the control result obtained using the open-loop-based extension method is presented. In the open-loop extension method, the steady-state gain of a controlled plant is required. Hence, $\boldsymbol{P}(1)$ is identified from two step responses of 50 s, where $\boldsymbol{u}(k)$ is set to $[1\ 0]^\top$ and $[0\ 1]^\top$, respectively:

$$\hat{\boldsymbol{P}}(1) = \begin{bmatrix} 0.463 & 0.537 \end{bmatrix}^\top \tag{30}$$

From the obtained steady-state gain, the add-on input is designed as follows:

$$w_o(k) = w_o(\infty) = 0.485 \tag{31}$$

The control result of the open-loop extension method is also shown in Figures 5–7, where the output and input trajectories are plotted by the blue dashed lines, and the sampled output trajectory is plotted by blue '$\diamondsuit$' symbols. It can be seen that when the steady-state gain of the controlled plant is available, the intersample ripple is eliminated

and the steady-state sampled response obtained by the conventional non-extension method is maintained.

4.2. Unstable Plant

As an unstable plant, the following transfer function is considered:

$$P(s) = \frac{1}{s^2 + 1.6s - 0.8} \tag{32}$$

The corresponding transfer functions in a dual-rate system are given as follows:

$$P_1(z^{-1}) = \frac{0.740 + 0.0403z^{-2}}{1 - 2.24z^{-2} + 0.0408z^{-4}}$$
$$P_2(z^{-1}) = \frac{0.332 + 0.392z^{-2}}{1 - 2.24z^{-2} + 0.0408z^{-4}}$$

The coefficients of the control law Equation (3) are designed as follows:

$$\boldsymbol{Y}(z^{-1}) = \begin{bmatrix} 1.0 + 0.0680z^{-2} & -0.100z^{-2} \\ 0 & 1 \end{bmatrix}$$
$$\boldsymbol{K}(z^{-1}) = \begin{bmatrix} 0.618 \\ 0.618 \end{bmatrix}$$
$$\boldsymbol{X}(z^{-1}) = \begin{bmatrix} 2.58 - 0.736z^{-2} \\ 1 \end{bmatrix}$$

where $\boldsymbol{G}(1)^\top \boldsymbol{K}(1) = 1$, and the poles of the closed-loop characteristic polynomial are 0.0696, 0.174 and -0.312.

The control result obtained by the non-extension control law with the coefficients designed as described above is shown in Figures 8–10, where the output and input trajectories are plotted by the black dashed-dotted lines, and the sampled output trajectory is plotted by black '*' symbols. As in the case of the stable plant, the intersample output oscillates even though the sampled output follows the reference input. The reason for this intersample oscillation is the oscillation of the control input, and $\boldsymbol{G}_r(1) = [-1.19 \quad -0.382]^\top$.

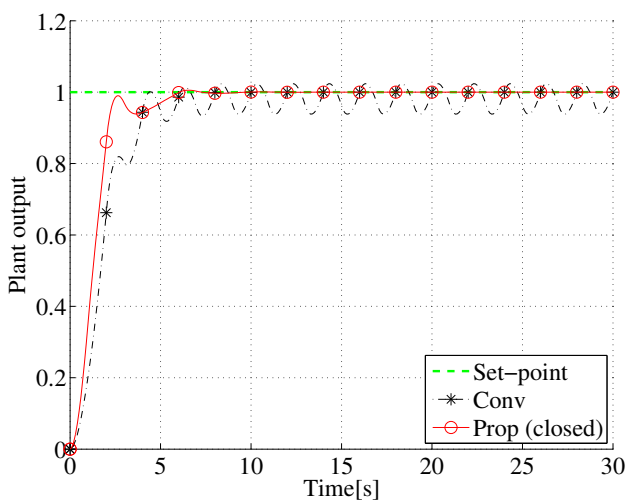

Figure 8. Output trajectories of unstable plant.

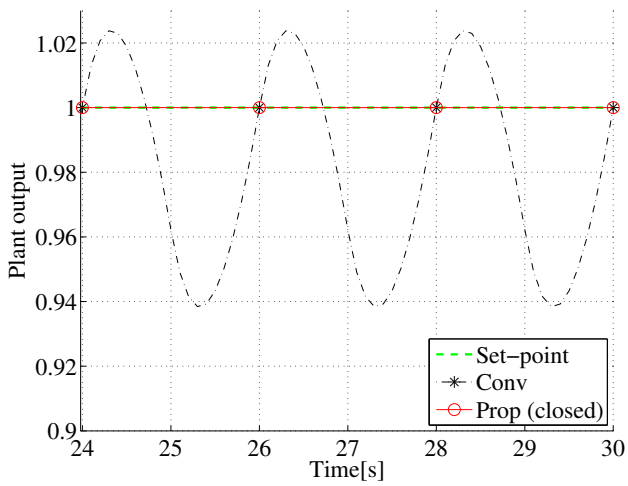

Figure 9. Steady-state trajectories for data in Figure 8.

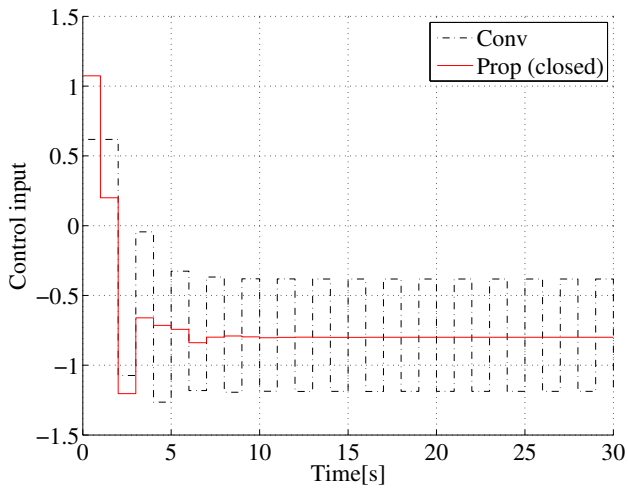

Figure 10. Input trajectories for unstable plant.

The open-loop-based method is not applicable to the unstable plant, whereas the proposed method is, because of the closed-loop-based design.

From two step responses of 30 s, the identified steady-state gain of the closed-loop system is given as follows:

$$\hat{\boldsymbol{G}}(1) = \begin{bmatrix} 0.774 & 0.844 \end{bmatrix}^{\top}$$

The corresponding orthogonal vector is given as follows:

$$\boldsymbol{G}_{\perp} = \begin{bmatrix} -0.737 & 0.676 \end{bmatrix}^{\top}$$

From Equation (20), the add-on input is obtained as follows:

$$w(k) = w(\infty) = -0.618$$

The control result obtained using the proposed method is shown in Figures 8–10, where the output and input trajectories are plotted by the red solid lines, and the sampled output trajectory is plotted by red '∘' symbols. As shown in Figures 8 and 9, the steady-state sampled output responses obtained by the conventional non-extension and proposed methods are the same. Furthermore, intersample ripple is eliminated using the proposed method.

The present study assumes that there will be no noise or disturbance, but in reality, there may be impacts. An example is shown where the output is disturbed by noise of variance 2.0×10^{-4}. Since the step response is affected by noise, the correct steady-state gain cannot be obtained:

$$\hat{\boldsymbol{G}}(1) = \begin{bmatrix} 0.863 & 0.968 \end{bmatrix}^{\top}$$

Therefore, the wrong orthogonal vector is given as follows:

$$\boldsymbol{G}_{\perp} = \begin{bmatrix} -0.747 & 0.665 \end{bmatrix}^{\top}$$

Simulation results in the presence of noise are shown in Figures 11 and 12, where the same noise is applied by fixing the seed value. Even when the proposed method is applied, the control input oscillates and intersample ripple is not eliminated.

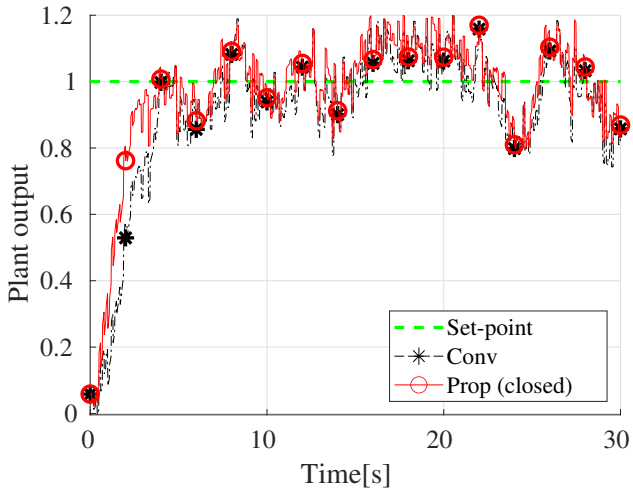

Figure 11. Output trajectories of unstable plant in the presence of noise.

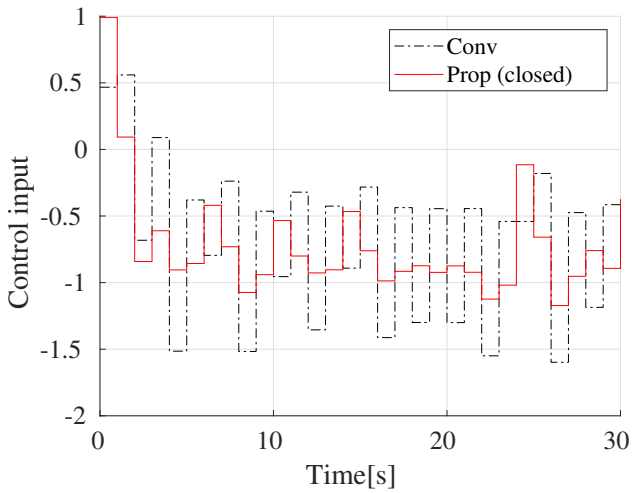

Figure 12. Input trajectories for unstable plant in the presence of noise.

5. Conclusions

The present study proposed a design method for a dual-rate sampled-data control system, in which the sampling interval is longer than the holding interval. In such a system, even when the sampled output converges to the reference input, the intersample output might oscillate because the control input may change between sampling instants. In the proposed method, an existing control law is extended by introducing an add-on input

based on the null space of step responses to eliminate intersample ripple independently of an existing steady-state sampled response. The proposed method is based on step responses and is easily implemented. Since the present study proposes the closed-loop-based method as well as the open-loop-based method, the proposed method can be applied to an unstable plant.

In the present study, the controlled plant is limited to linear time-invariant systems; however, the proposed method can be applied to wider classes. The proposed method is applicable when the steady-state output is uniquely determined for the steady-state input, but difficult otherwise. Therefore, our future work is to clarify the class of controlled plants in which the proposed add-on design method is applicable. The present study assumes the case where there is no unknown information such as noise. Therefore, it is necessary to deal with cases where the steady-state gains cannot be estimated correctly due to disturbances and so on. In addition, verification using actual equipment is also an issue for the future. Furthermore, in the present study, the add-on input is designed so that the intersample response is improved in the steady state. Therefore, one of the future works is to design the add-on input to improve the transient response as well as the steady-state response.

Author Contributions: Conceptualization, T.S. and R.Y.; methodology, T.S., R.Y. and N.K.; software, T.S. and R.Y.; validation, N.K.; formal analysis, T.S., R.Y. and N.K.; investigation, T.S. and N.K.; resources, T.S. and N.K.; data curation, T.S., R.Y. and N.K.; writing—original draft preparation, T.S. and R.Y.; writing—review and editing, T.S. and N.K.; visualization, T.S., R.Y. and N.K.; supervision, T.S.; project administration, T.S.; funding acquisition, T.S. and N.K. All authors have read and agreed to the published version of the manuscript.

Funding: This research received no external funding.

Institutional Review Board Statement: Not applicable.

Informed Consent Statement: Not applicable.

Acknowledgments: The present study was supported by the Suzuki Foundation.

Conflicts of Interest: The authors declare no conflict of interest.

References

1. Chen, T.; Francis, B. *Optimal Sampled-Data Control Systems*; Springer: London, UK, 1995.
2. Åström, K.J.; Wittenmark, B. *Computer-Controlled Systems: Theory & Design*, 3rd ed.; Prentice Hall: Upper Saddle River, NJ, USA, 1997.
3. Araki, M.; Hagiwara, T. Pole assignment by multirate sampled-data output feedback. *Int. J. Control* **1986**, *44*, 1661–1673.
4. Araki, M.; Yamamoto, K. Multivariable Multirate Sampled-data Systems: State-space Description, Transfer Characteristics, and Nyquist Criterion. *IEEE Trans. Autom. Control* **1986**, *31*, 145–154.
5. Salt, J.; Albertos, P. Model-Based Multirate Controllers Design. *IEEE Trans. Control Syst. Technol.* **2005**, *13*, 988–997.
6. Jia, Y.; Chai, T. A data-driven dual-rate control method for a heat exchanging process. *IEEE Trans. Ind. Electron.* **2016**, *64*, 4158–4168.
7. Carini, P.; Micheli, R.; Scattolini, R. Multirate self-tuning predictive control with applications to binary distillation column. *Int. J. Syst. Sci.* **1990**, *21*, 51–64.
8. Zhang, B.; Zhou, K.; Wang, D. Multirate Repetitive Control for PWM DC/AC Converters. *IEEE Trans. Ind. Electron.* **2014**, *61*, 2883–2890.
9. Furusaka, T.; Sato, T.; Kawaguchi, N.; Araki, N.; Konishi, Y. Consensus Control of Dual-rate Multi-agent Systems with Quantized Communication. *IEEE Access* **2020**, *8*, 97557–97563.
10. Chen, B.M.; Lee, T.H.; Venkataramanan, V. *Hard Disk Drive Servo Systems*; Springer: Berlin/Heidelberg, Germany, 2002.
11. Mamun, A.A.; Guo, X.; Bi, B. *Hard Disk Drive; Automation and Control Engineering*; CRC Press: Boca Raton, FL, USA, 2007.
12. Salt, J.; Tomizuka, M. Hard disk drive control by model based dual-rate controller. Computation saving by interlacing. *Mechatronics* **2014**, *24*, 691–700.
13. Li, D.; Shah, S.; Chen, T. Analysis of Dual-Rate Inferential Control Systems. *Automatica* **2002**, *38*, 1053–1059.
14. Sato, T.; Kusakabe, T.; Himi, K.; Araki, N.; Konish, Y. Ripple-free Data-driven Dual-rate Controller Using Lifting Technique: Application to a Physical Rotation System. *IEEE Trans. Control Syst. Technol.* **2021**, *29*, 1332–1339.
15. Moore, K.; Bhattacharyya, S.; Dahleh, M. Capabilitied and Limitations of Multirate Control Schemes. *Automatica* **1993**, *29*, 941–951.
16. Sheng, J.; Chen, T.; Shah, S.L. Multirate Generalized Predictive Control for Sampled-Data Systems. *Dyn. Contin. Discret. Impuls. Syst. Ser. Appl. Algorithms* **2001**, *8*, 485–499.

17. Ishitobi, M.; Kawanaka, M.; Nishi, H. Ripple-Suppressed Multirate Adaptive Control. In Proceedings of the 15th IFAC World Congress, Barcelona, Spain, 21–26 July 2002; pp. 327–332.
18. Salt, J.; Sandoval, J.; Albertos, P. Dual-Rate Control Ripple Detection by an Approximate Frequency Respoinse Methodology. In Proceedings of the Fourth IEEE Congress of Electronics, Robotics, and Automotive Mechanics, Cuernavaca, Mexico, 25–28 September 2007; pp. 89–94.
19. Oomen, T.; van de Wijdeven, J.; Bosgra, O. Suppressing intersample behavior in iterative learning control. *Automatica* **2009**, *45*, 981–988.
20. Tangirala, A.; Li, D.; Patwardhan, R.; Shah, S.; Chen, T. Ripple-Free Conditions for lifted Multirate Control Systems. *Automatica* **2001**, *37*, 1637–1645.
21. Jia, Q.; Oooi, K.; Wu, D. Multirate Control of an HDD Servo System with Intersample Ripple Free. *IEEE Tran. Megnetics* **2002**, *38*, 2192–2194.
22. Atsumi, T.; Messner, W.C. Mixed Sensitivity Problem in Sampled-Data Positioning Control Systems. *J. Syst. Des. Dyn.* **2011**, *5*, 1294–1309.
23. Inoue, A.; Sato, T.; Deng, M.; Yanou, A. A Multi-rate Optimal Controller to Suppress Ripples at Transient State. In Proceedings of the 2018 IEEE International Conference on Systems, Man, and Cybernetics, Miyazaki, Japan, 7–10 October 2018; pp. 2641–2646.
24. Sato, T. Parametric Design of a Dual-Rate Controller for Improvement in Steady-State Intersample Response. *SICE J. Control Meas. Syst. Integr.* **2008**, *1*, 329–334.
25. Zaccarian, L. Dynamic Allocation for Input Redundant Control Systems. *Automatica* **2009**, *45*, 1431–1438.
26. Sato, T.; Kawaguchi, N.; Araki, N.; Konishi, Y. Ripple-Free Design for an SISO Dual-Rate Control System. In Proceedings of the 22th IEEE International Conference on Emerging Technologies and Factory Automation, Limassol, Cyprus, 12–15 September 2017.
27. Yasui, R.; Kawaguchi, N.; Sato, T.; Araki, N.; Konishi, Y. Dual-Rate Control System Extension Using the Null-Space of Closed-loop System. *IEEJ Trans. Electr. Electron. Eng.* **2020**, *15*, 135–139.
28. Yasui, R.; Kawaguchi, N.; Sato, T.; Araki, N.; Konishi, Y. Steady-State Dual-Rate Open-Loop Transfer Function Model-Based Ripple-Free Design. *IEEJ Trans. Electr. Electron. Eng.* **2021**, *16*, 1435–1437.
29. Sato, T.; Sakai, Y.; Kawaguchi, N.; Arrieta, O. Dual-Rate Data-Driven Virtual Reference Feedback Tuning: Improvement in Fast-Tracking Performance and Ripple-Free Design. *IEEE Access* **2021**, *9*, 144426–144437.